

Locomotion of Mexican jumping beans

Daniel M West¹, Ishan K Lal¹, Michael J Leamy¹ and David L Hu^{1,2,3}

¹ School of Mechanical Engineering, Georgia Institute of Technology, Atlanta, GA 30332, USA

² School of Biology, Georgia Institute of Technology, Atlanta, GA 30332, USA

E-mail: hu@me.gatech.edu

Received 29 October 2011

Accepted for publication 12 April 2012

Published 10 May 2012

Online at stacks.iop.org/BB/7/036014

Abstract

The Mexican jumping bean, *Laspeyresia saltitans*, consists of a hollow seed housing a moth larva. Heating by the sun induces movements by the larva which appear as rolls, jumps and flips by the bean. In this combined experimental, numerical and robotic study, we investigate this unique means of rolling locomotion. Time-lapse videography is used to record bean trajectories across a series of terrain types, including one-dimensional channels and planar surfaces of varying inclination. We find that the shell encumbers the larva's locomotion, decreasing its speed on flat surfaces by threefold. We also observe that the two-dimensional search algorithm of the bean resembles the run-and-tumble search of bacteria. We test this search algorithm using both an agent-based simulation and a wheeled Scribbler robot. The algorithm succeeds in propelling the robot away from regions of high temperature and may have application in biomimetic micro-scale navigation systems.

 Online supplementary data available from stacks.iop.org/BB/7/036014/mmedia

(Some figures may appear in colour only in the online journal)

1. Introduction

Mobile rolling robots are a unique design for locomotion and have long attracted the attention of roboticists (Wang and Halme 1996, Bhattacharya and Agrawal 2002, Sugiyama *et al* 2006, Alves and Dias 2003). This design has two main benefits: (1) a hard spherical shell protects the robot's components from hostile environments and (2) a round shape enables the robot to utilize rolling locomotion, which is highly efficient on smooth surfaces. A review of recent progress toward building and controlling spherical and cylindrical rolling robots is given by Armour and Vincent (2006). The motivation of the current work is to contribute to robotics through investigation of a related type of locomotion found in biology. We here use the Mexican jumping bean as a model organism for rolling locomotion within an armored shell.

The Mexican jumping bean (figures 1(a) and (a')) consists of a brown seed capsule animated by a parasitic moth larva. In popular culture, the beans are used as children's toys and in games of chance because of their seemingly random motion. The underlying hypothesis of this study is that although the

hard shell protects the larva from the elements, it impedes navigation, locomotion and sensation of its environment.

Mexican jumping beans originate from the northwestern mountains of Mexico, including the Sonoran desert. Their life cycle consists of several stages (Heckrotte 1983), beginning with the moth *Laspeyresia saltitans* laying its eggs in the flowers of the fern *Sebastiania pavoniana* in early summer. The flowers mature into pie-shaped seed pods, which in turn split apart to entrap moth larvae in carpals resembling slices of a pie (figure 1(a')). The seed pods, or 'beans', drop from the fern following mid-summer rains, after which they must quickly seek out shadows and crevices in which to hide from the Mexican sun. Temperatures where the beans are found have a wide range in the summer months, ranging from 0 °C at night to up to 56 °C in the shade. To escape the highest temperatures, the bean continues to seek shelter for six to eight months, but with decreasing vigor as the larva matures. The larva's last act before pupation is to cut a round trapdoor in the seed, which it uses to exit the seed after transforming into an adult moth.

In our investigation, we will discuss the motion of the larva in either of two states: (1) enclosed within its bean shell, a state that we refer to it as the *bean* or (2) outside its bean shell, a state that we refer to as the *larva*. The means by which the larva

³ Author to whom any correspondence should be addressed.

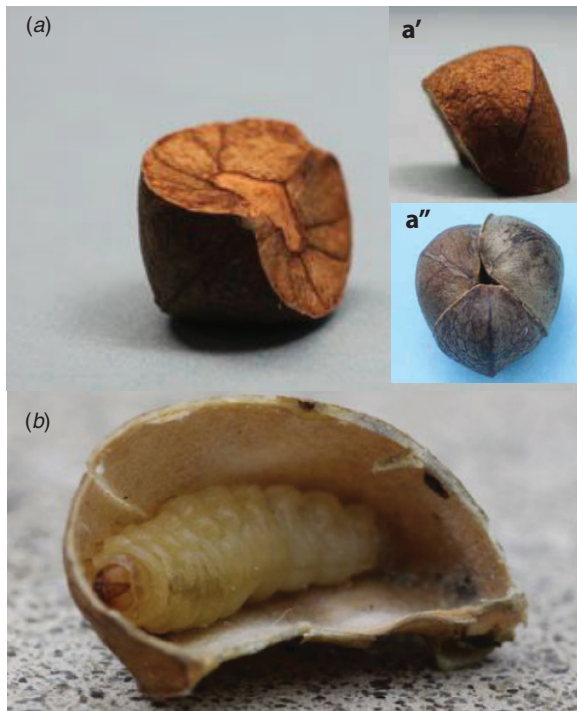


Figure 1. The Mexican jumping bean. (a) Orientation of the bean with round side down, and (a') flat side down. (a'') Three beans forming a complete seed pod. (b) The bean, cut in cross-section showing the larva and the web it has built inside the seed pod.

controls its encasing seed pod was first elucidated by Herter (1955). By placing the larva inside a transparent pill capsule, Herter found that the larva attaches itself to the capsule with silk threads. The motion of the bean is actuated by rocking the threads in one of two ways. If the larva walks around the inside surface of the capsule, rolling occurs. Jumping is made possible by the larva grabbing the shell with its posterior prolegs and rapidly striking the capsule with its other end. In section 4, we report the probability distribution of each of these movements.

Quantitative experiments of the bean's response to temperature were conducted by Heckrotte (1983). The author showed that jumping beans have an internal timer that modulates the frequency and duration of their movements, subject to temperature. For example, at 30 °C, the beans will exhibit a period of high activity, jumping 30 times per minute for a duration of 15 min. Afterward, the bean enters a period of hibernation lasting up to 24 h. Heckrotte found that the frequency of movements increased with increasing temperature, peaking at 40 movements per minute at 45 °C.

In this study, we report the results of a combined experimental, numerical and robotic investigation of jumping bean locomotion. We begin in section 2 with a discussion of preliminary theoretical considerations, namely the limits of motion for spherical robots as found by previous investigators. In section 3, we present the experimental, numerical and robotic methods used in this study. In section 4, we present our experimental results of our survey of bean locomotion, including the trajectories of beans in channels and along inclines. In section 5, we present our robotic and numerical

results, demonstrating that we have captured the essence of the bean sensing and motion both in a simple robot and *in silico*. In section 6, we discuss the implications of our work and suggest directions for future research.

2. Preliminary theoretical considerations

We first consider a few simple mechanical principles that constrain the jumping bean's motion. The propulsion of the bean is similar to that of spherical robots in that locomotion is generated by the motion of an imbedded mass or driver (Wang and Halme 1996). For the beans, the larva walking inside the shell causes it to tip over and roll.

The larva is 1 cm long and has a characteristic mass of $m = 0.05$ g (where the number of insects measured is $N = 12$). Without the larva, the shell has mass $M_{\text{shell}} = 0.05$ g nearly equal to that of the larva. Approximating the shell as spherical, it has a characteristic radius $R \approx 0.5$ cm and thickness $b = 0.1$ cm. When the larva walks up the inner surface of the shell, its weight applies a torque around the shell's point of contact with the ground. This torque causes the spherical shell to roll. The angular acceleration α of the shell with larva is

$$\alpha = \frac{3}{2} \frac{m}{M_{\text{shell}}} \frac{g \sin \theta}{R}, \quad (1)$$

where θ is the angle shown in the inset of figure 2(a) and g is the gravity. Since the acceleration of the shell is proportional to the ratio of mass of larva to shell, the larva should employ a lightweight shell to roll quickly. The characteristic timescale for the rolling is thus given by $\Delta t \sim \sqrt{\frac{M_{\text{shell}} R}{mg}} \approx 0.023$ s, which is small compared to the time it takes for the larva to walk up the shell (on the order of 0.5 s). By rolling inside its shell, the larva can travel at burst speeds of 2.0 cm s^{-1} , which is four times higher than its peak walking speed (0.5 cm s^{-1}).

The largest incline angle γ that a spherical shell can climb was first derived by Wang and Halme (1996) and is given by

$$\gamma_{\text{max}} = \sin^{-1} \left(r/R - \frac{\kappa}{R} - \frac{\kappa M_{\text{shell}}}{mR} \right), \quad (2)$$

where r is the radial position of the larva's center of mass and $\kappa \approx 0.15$ cm is the coefficient of rolling friction (for wood on wood (Avallone *et al* 2007)). The width W of the larva is 0.3 cm; yielding an $r = R - W/2 = 0.35$. Using the remaining values for the jumping bean geometry and mass, we predict that the maximum incline angle for a spherical bean is $\gamma_{\text{max}} = 5^\circ$. In reality, this value is highly dependent on the shape of the bean, as we shall see in our results.

The largest obstacle the shell can climb is given by (Wang and Halme 1996)

$$h_{\text{max}} = R - \sqrt{R^2 - \left(\frac{mR - \kappa(m + M_{\text{shell}})}{M_{\text{shell}} + m} \right)^2}. \quad (3)$$

Using our measurements of shell mass and radius, we find that a spherical bean could traverse obstacles $h_{\text{max}} = 0.02$ mm in height. In reality, the asymmetric shape of the shell allows it to cross obstacles that are nearly 1 cm in height.

One drawback of containment within a shell is the longer time required by the larva to sense its ambient temperature. This time lag negatively affects navigation because the larva

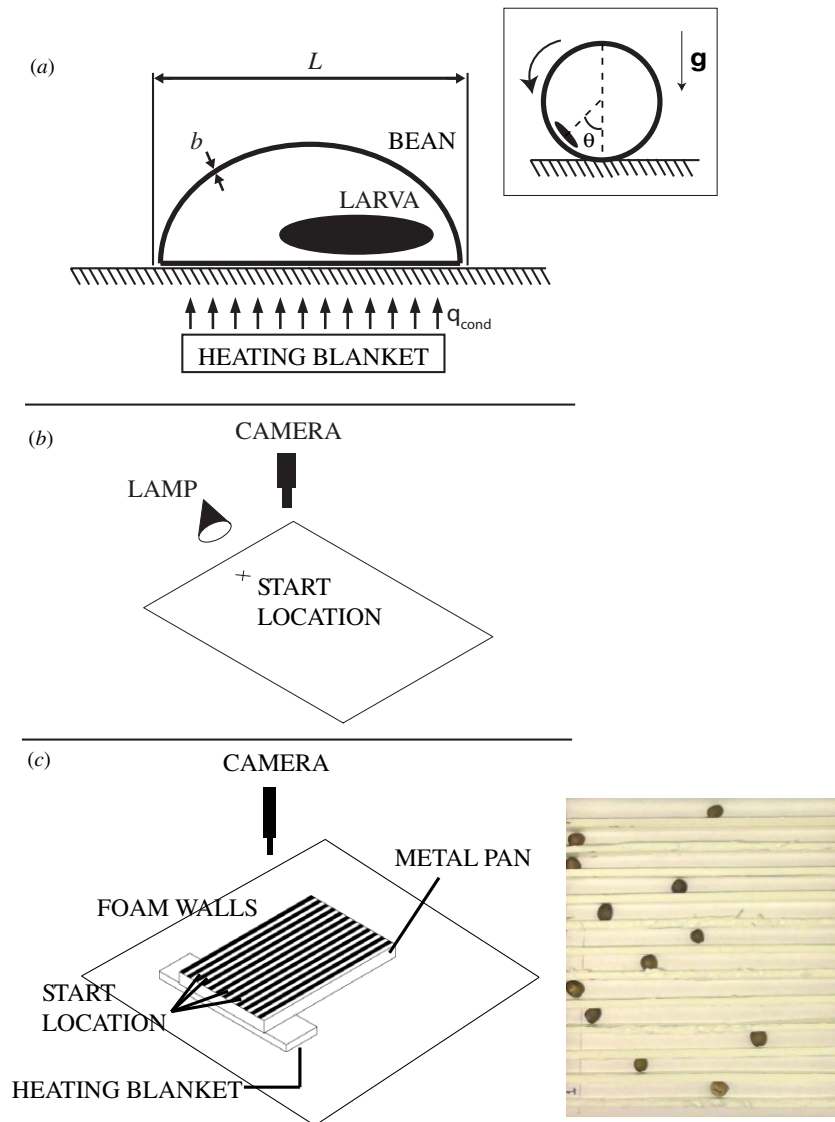


Figure 2. (a) Schematic of the jumping bean atop a heated surface. (b) Experimental setup for observing bean motion on planar surfaces. (c) Experimental setup for observing bean motion in 1D channels. The apparatus made from metal tray and foam board can be used to observe 12 beans or larvae simultaneously (see inset). The apparatus can be tilted at an angle ϕ with respect to the horizontal to observe the motion of the bean up inclines.

bases its direction of movement on sensation of its surrounding temperature. The time constant for sensing a temperature T can be approximated using Fourier's law (Incropera *et al* 2007) (figure 2(a)),

$$\rho V c \frac{dT}{dt} = -k A \nabla T, \quad (4)$$

where ρ and c denote the density and specific heat of the shell material, V is the volume of the bean, A is the area in contact and k is the conduction coefficient. Non-dimensionalizing this equation with a timescale τ and length scale b , given by the thickness of the shell, we find that the timescale of heat is $\tau_{\text{sense}} = \frac{b\rho V c}{kA}$. Using the appropriate values of c (4000 and 1000 J (kgK)⁻¹) and k (0.12 and 0.6 W (mK)⁻¹) for wood and water, respectively (Incropera *et al* 2007), we find that the shell requires 1 s to heat up and the larva 10⁻¹ s. Thus, according to these estimates, the larva can sense surroundings

temperature ten times faster outside of the shell than from inside.

A greater sensitivity clearly allows the larva to react to its environment more quickly than the bean. However, there may be potential sensing benefits for the bean's shell in certain environments. For instance, the higher heat capacity of the bean shell acts both as an integrator and as a low-pass filter for temperature. This might enable it to disregard misleading changes to the radiation, convection or conduction of its surroundings, such as by a breeze or a passing shadow.

3. Methods

We studied the movements of jumping beans using a combination of experimental, numerical and robotic methods, which we present here. We begin with a description of methods for bean care and motion recording.

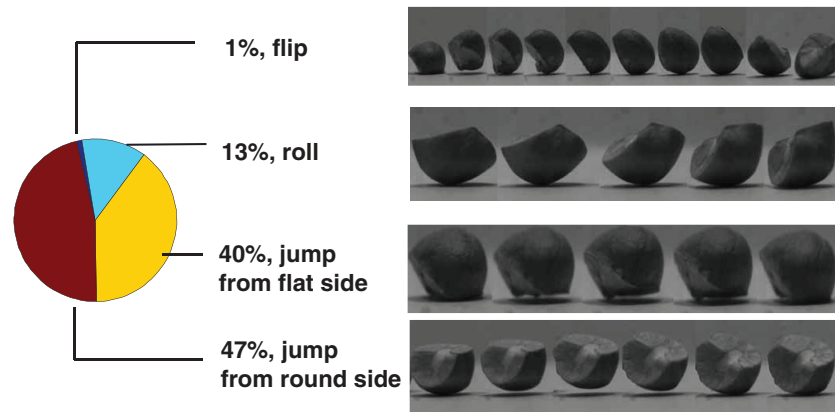


Figure 3. High-speed film sequences of the jumping beans movements, including rolls, jumps and flips. The frequency of maneuvers is shown.

3.1. Jumping beans

3.1.1. Bean care and observations. Mexican jumping beans were procured from the professional breeder MyPetBeans.com. Beans were kept dormant by refrigeration at 5 °C, which is below their minimum active temperature of 10 °C. Keeping the beans dormant during non-testing extended the lifetime of the larvae for up to two months. Larvae were removed from the shell with a pen knife and once outside the seed they were used for up to one day of experiments. Keeping the larvae outside of the shell for longer durations significantly decreased both their movement and their life expectancy (to 2–3 days). Bean movements (figure 3) were categorized using observations of ten beans at a uniform room temperature for a 10 min period on a planar cardboard surface. Video recordings were made using a Sony HD HandyCam and a high-speed Phantom V10 camera.

3.1.2. Two-dimensional (2D) tests. Qualitative testing was performed using five beans atop a planar surface with a radial temperature gradient. A white cardboard sheet (0.6 m × 0.6 m) was illuminated by a desk lamp (25 W halogen) as shown in figure 2(b). A temperature gradient of 0.54 °C cm⁻¹ was recorded using a handheld infrared thermometer (Kintrex IRT0421 non-contact infrared thermometer with an accuracy of 1 °C for the temperature range tested). Beans were initially placed flat side down underneath the spotlight. The subsequent 10 min of motion were filmed and digitized using MATLAB. Following filming of the bean, the larva was removed from the shell and subjected to the same procedures.

3.1.3. One-dimensional (1D) tests. Quantitative testing was performed using 12 beans tested on a 12 lane desktop racetrack as shown in figure 2(c) and in the supplementary movie, available from stacks.iop.org/BB/7/036014/mmedia. The apparatus consisted of a metal baking pan, whose bottom was lined with paper and lanes divided by foam-board walls. Heat was applied to one end of the track using an electric heating blanket under the pan. The apparatus provided each lane with near-identical start temperatures. We tested three temperature gradients (low, medium and high) corresponding

to maximum temperatures of 34, 37 and 40 °C and average temperature gradients of 0.59, 0.79 and 0.99 °C cm⁻¹. The highest temperature gradient had a parabolic distribution ($T = 0.06x^2 - 2.0x + 41$, where x is in cm and T in °C), as verified with infrared thermometer. Bean tests were performed for 5 min in duration at all three temperature settings. Twelve beans were raced along the racetrack for six trials; then the shells were cut open and the larvae were each run for six trials. Beans were placed with a starting orientation of flat side down; larva were placed leg-side down and facing the finish line of the track. Tests were also run to measure the bean's ability to move up an incline (with angles between 0° and 15° and increments of 2.5°).

3.2. Robot and simulation

We wrote an algorithm of jumping bean behavior as a means for (1) implementing our findings on thermotaxis robotically and *in silico*, (2) testing hypotheses about the overarching rules governing bean behavior and (3) exploring emergent bean behavior in complex environments where similar experimental studies become too labor intensive to plan and execute. The algorithm may be of further utility in the future as a means for exploring the effectiveness of biomimetic concepts which base their behavior on jumping bean thermotaxis.

The robot code was written in Python. The agent-based algorithm was written using the NetLogo simulation software and a copy of the code is available in the supplementary information, available from stacks.iop.org/BB/7/036014/mmedia. The application to run the software is available free online.

3.2.1. Robot. The jumping bean search algorithm was tested using the robot shown in figure 8(a). We modified a wheeled Scribbler robot developed by Parallax, Inc. to sense light, turn and move forwards. The robot consisted of three light sensors and two independent DC motors (to drive the wheels). The robot's pen port facilitated tracking the robot's trajectory.

The robot was programmed such that it moved toward lower light intensity values. The robot had two phases of motion. In the 'tumble' phase, the robot rotated 360° while

sensing light intensity values from its photo sensors on board and storing the data values at each 45° turn, resulting in eight measurements per tumble. The robot calculated the minimum light value among these eight readings and turned toward the lowest light intensity direction. Consistent with the optimal results found in our computational model, we programmed the robot to perform its tumble toward clockwise and counter-clockwise with equal probability. In the ‘run’ phase, the robot moves a preset distance toward the direction with the lowest light intensity value. For our testing, we assumed that higher light intensities equated to a higher temperature.

An important design consideration in building the robot was repositioning its light sensors. The position of the IPRE fluke board was changed in order to align the photo sensors to face the top (light source). Without this modification, the robot’s own shadow would interfere with its light sensing ability.

The robot walk algorithm was run and tested under a radial light gradient created by a halogen lamp mounted vertically above the floor of a darkened room. Our light source was a fluorescent desk lamp with a GE 13 W bulb held at a distance to the ground of 40 cm. Our light sensors detected light 7.5 cm above the ground. Robots placed in this radial gradient were easily capable of finding their way toward the darkest parts of the room. A trace of the robot’s motion was recorded on paper using the pen port of the robot and is shown in figures 8(b) and (c).

3.2.2. Simulation. The computational model was developed using the *NetLogo* agent-based simulation software (Wilensky 1999). Agent-based models (ABMs) are particularly attractive for capturing the collective, emergent, behavior of individuals operating in a complex and stochastic environment. Prevalent examples include the simulation of markets or economies, traffic congestion, warfare, population dynamics and disease spread. In each of these scenarios, the simulation embodies a collection of mobile, autonomous agents operating on a uniformly gridded, or celled, landscape. This can be viewed as cellular automata (Wolfram 2005) with the inclusion of mobile agents, where both the cells and the agents store a set of states. The autonomous agents make decisions about their next position based on a set of rules which account for the agent’s state, its neighboring agents’ states and the states of the cellular landscape in close proximity to the agent. Time therefore flows in an explicitly stepped manner in which each agent evaluates its next move before the simulation proceeds to the next time step. Along with updates of agent positions, there are updates to the agents’ state variables during each step. An in-depth review of agent-based modeling is given by Bonabeau (2002).

The ABM modeling paradigm works well in studying jumping bean thermotaxis on a plane. The landscape can be easily programmed to hold a temperature distribution, and the agents can be used to represent the jumping bean larvae with or without the bean shell. The only state held by either a cell or an agent (i.e. bean) is its temperature. The agents also store a non-state variable specifying their desired temperature (i.e. the temperature they would like to achieve, above which they

Table 1. Duration and distance traveled for each bean motion. Averages and standard deviations are measured for three beans.

	Roll	Jump	Flip
Duration (s)	0.2 ± 0.03	0.04 ± 0.02	0.4 ± 0.2
Distance (cm)	0.5 ± 0.1	1 ± 0.4	3 ± 1

seek cooler surroundings). Simple rules can then be specified which determine the temperature update of the beans at the next time step, and which determine their next position.

4. Experimental results

4.1. Bean movement types: roll, jump and flip

Using high-speed video, we categorized the movements of the bean (see supplementary video, available from stacks.iop.org/BB/7/036014/mmedia, and figure 3). The geometry of the bean is visibly asymmetric (figure 1), which governs the range of movements that are possible. The bean can stably remain at rest upon either of its two flat faces or upon the apices of its two hemispherical surfaces. After observing many bean motions, we categorized the possible motions into three distinct actions: roll, jump and flip. In the first type of movement, the bean simply changes orientation by rolling across one of its ridges. In the second type of movement, called the ‘jump’, the bean is airborne for a brief period as it hops, but lands upon the same face from which it jumped. In the last type of movement, the ‘flip’, the bean performs a vigorous leap to land on a different one of its faces. The duration and distance traveled for each type are shown in table 1. Flips travel the greatest distance followed by jumps and then rolls.

The energy used by the larva to jump and flip can be estimated by the maximum gravitational energy $E = (m + M_{\text{shell}})gh$ achieved, where h is the change in height of the center of mass. Since the height of the jump is 0.1 cm, while the height of the flip is 0.75 cm, we conclude that the flip requires 75 times more energy than the jump. Our measurements of the frequency of these movements match well with these energetic costs. Figure 3 shows the frequency distribution of rolls, jump and flips for a total number of 550 movements by ten beans. Consistent with the relative energies associated with each motion, the bean jumps 85% and flips 1% of the time. The remaining 14% of the time were rolls in which the bean would simply pivot along its ridge.

A simple drop test was performed to determine if the bean’s geometry or mass distribution gave it an affinity for the flat or round side. The beans were dropped from a height of 10 cm. Over 120 trials, the bean landed with nearly equal probability on the flat and round sides (62 versus 58), indicating there is no bias in landing probability.

4.2. Run-and-tumble trajectories

To visualize the paths made by the beans to escape heat, we filmed the trajectories of the beans on flat surfaces and in 1D racetracks. For the former, figure 4 shows the planar paths of

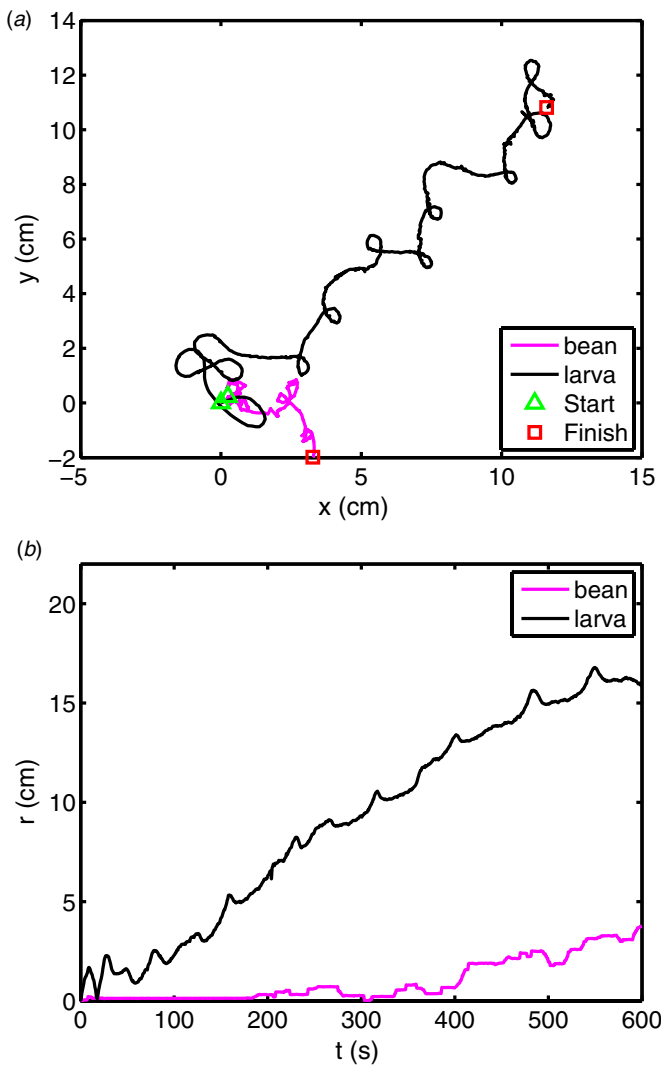


Figure 4. (a) The 2D trajectories of bean and larva exposed to a radial temperature gradient. (b) The time course of the radial distance traveled from the start position.

the bean and larva for a duration of 10 min. Figure 4(b) shows the time course of the radial distance r traveled from the start position. The periodic tumbling of the bean and larva occurs at 30 s intervals. Both bean and larva manage to move away from the heat source, but the larva travels three times faster, as shown by the longer distance traveled. Both trajectories are characterized by a series of runs and loops, analogous to the run and tumble of bacteria (Berg 1993) or the circular trajectories of humans when lost (Souman *et al* 2009). In this case, a ‘tumble’ is actuated by the larva walking in a circle of 0.5 cm diameter. In reality, the larva travels in smooth loops which can be either left or right handed. We will explore how these tumble types affect the efficacy of thermotaxis in our numerics in the next section.

Our 1D tests further confirm that beans exhibits a run-and-tumble trajectory. Figure 5(a) shows the time course of the position of three beans under a temperature gradient of $1.36\text{ }^{\circ}\text{C cm}^{-1}$. The beans’ motion can be divided into three stages. In the first stage, lasting 1–1.5 min, the bean holds its position: specifically, the bean remains within 2 cm of the origin despite

rapid oscillations every few seconds. In the second stage, the bean progresses forward into cooler regions at a high speed (up to 20 bean lengths per minute). This stage is interrupted every 30 s, when the bean appears to be checking its bearings (by oscillating back and forth). The final stage is characterized by a plateau in movement at the preferred temperature of the bean, shown by their fixed position on the racetrack. Beans generally arrive at this preferred temperature within 2 min of the start of the test.

Based on the presence of a plateau stage, we conclude that variation in bean speed (averaged over 10 min) arises from variation in their preferred temperatures. Thus, although jumping beans are used in games of chance, their individual motions are largely deterministic. Randomness in jumping bean games occurs in two places: in the bean’s tumbling (left or right) and in the player’s random selection of which bean to use. Each bean has its own preferred temperature.

Figure 5(b) shows the relation between temperature gradient ($^{\circ}\text{C cm}^{-1}$) and the average dimensionless speed traveled by the bean over 10 min. As expected, the beans move faster at the highest temperature gradients tested ($dT/dx = 1^{\circ}\text{C cm}^{-1}$). The large error bars are consistent with the large variability in bean preferred temperature.

The bean’s asymmetrical shape allows for improved climbing ability compared with respect to a spherical shape. The heat source and the beans were placed upon inclines of $\gamma = 0\text{--}15^{\circ}$ at 2.5° increments. Figure 6 shows the relation between climbing speed and incline angle. As expected, the beans decreased speed with increasing incline angle, in accordance with the greater energy required to climb up steeper slopes. The maximum incline angle climbed was $\gamma_{\text{max}} \approx 9\text{--}15^{\circ}$. This angle is larger than the angle calculated in section 2 for a spherical bean with the same mass and size as the jumping bean. We attribute this improved climbing ability to the flat sides of the bean, which prevent undesired rolling and allow the bean to act as a ratchet.

5. Robot and simulation results

To further study the run-and-tumble trajectory performed by the beans, we idealize this algorithm and test its efficacy in both a robot and simulation. The algorithm, given in symbolic flow chart format in figure 7, allows for comparison of candidate rule sets in capturing emergent bean behavior. Once a representative rule set has been determined, we can explore bean behavior in more complex environments.

Input parameters for the simulation allow multiple beans to be simulated (*num-beans*) and specification of the initial bean temperature to start the simulation (*initial-bean-temp* $T(0) = 65$), the temperature at which each bean stops moving (*happy-bean-temp* = 17), a lumped heat transfer coefficient ($\bar{h} = 0.1$), the number of run steps the bean takes before performing a tumbling/turning maneuver (*run-steps-before-tumble* = 20), and the accuracy with which the beans can sense the landscape temperature (*sensing-accuracy* S). The lumped heat transfer coefficient arises from a discrete version of equation (4) given by

$$T(k+1) = T(k) - \bar{h}(T(k) - T_{\text{cell}}), \quad (5)$$

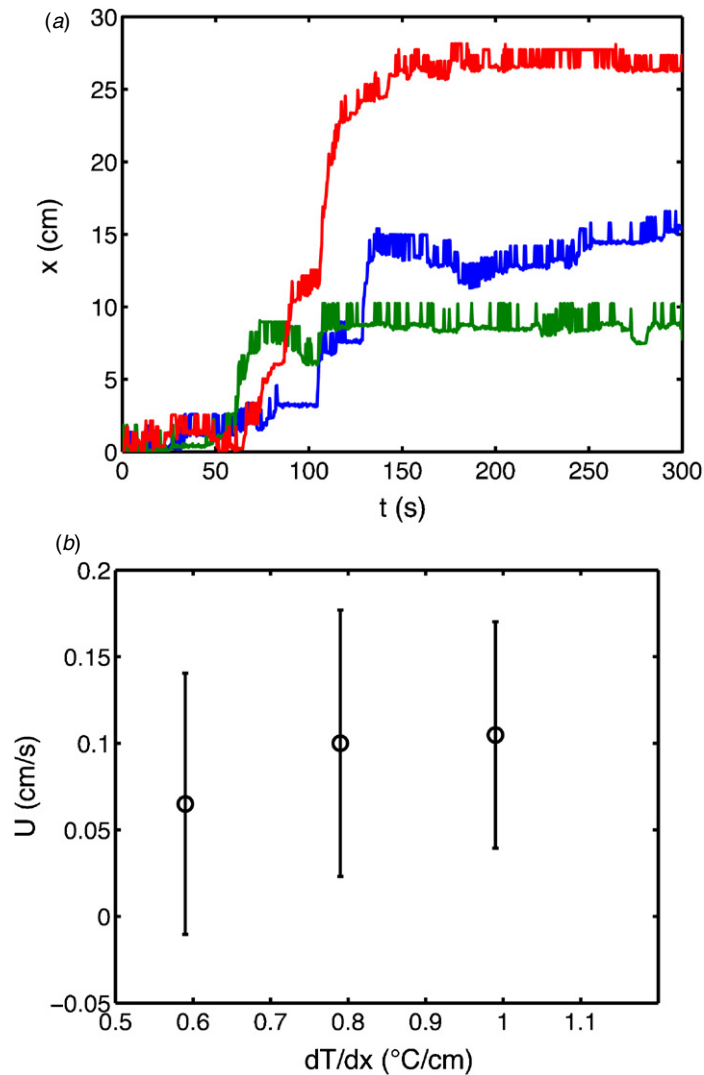


Figure 5. Bean tracking for a 1D channel. (a) The time course of the distance traveled for three typical beans (red, green and blue) under the temperature gradient $0.54\text{ }^{\circ}\text{C cm}^{-1}$. (b) The relation between temperature gradient and speed of the bean.

where $T(k)$ denotes the bean's temperature at time step k and T_{cell} denotes the temperature of the cell occupied by the bean at time step f . Comparison of equation (5) to (4) yields an expression for *heat transfer-coeff* $\bar{h} = \frac{kA}{\rho V c} \Delta t$, where Δt denotes the simulation time step.

A sensing-accuracy parameter S acts to modify the cell temperature measured by a bean as follows:

$$T_{\text{sensed}} = T_{\text{cell}} + \frac{0.5 - R[1.0]}{0.5} \left(1.0 - \frac{S}{100.0} \right) T_{\text{cell}}, \quad (6)$$

where $R[1.0]$ denotes the result of generating a uniform random number between 0 and 1.0, T_{sensed} is the temperature sensed and registered by the bean. This is one choice for introducing sensing error which we will denote as proportional sensing accuracy; another easily implemented choice could include a non-proportional sensing accuracy whereby the bean is assumed to have a fixed temperature sensing variance independent of the temperature it is trying to sense. In the computational model, the bean uses *sensed-temp* during tumbling maneuvers to ultimately determine the next best

direction to head toward. In our robot, we assume a sensing accuracy of 1.

A radial temperature distribution is assumed for the landscape (shown to the right of the parameter input) with a specified center temperature (*center-temp* = 65) and a radial temperature gradient ($dT/dr = \text{temp-gradient} = -0.5$) that is generally negative. This gradient acts to change the temperature in the radial direction by the specified quantity over one cell length. We used this landscape because for this case, it is clear that optimal behaviors of the bean are purely radial motions from the origin. Here we define an optimal trajectory as the one that results in the absolute minimum number of bean movements necessary for the bean to achieve its desired temperature.

The testing landscape consists of a grid of 250×250 cells. In our code, depressing of the *setup* action populates the landscape with beans and establishes the temperature distribution, while depressing the *go* button starts and stops the simulation. The beans are all assumed to start at the center of

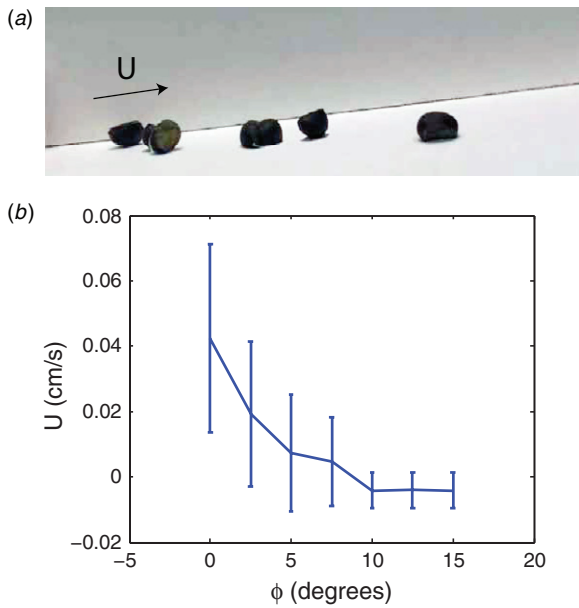


Figure 6. (a) Time-lapse video of a bean moving up an inclined plane is shown. (b) The relation between incline angle ϕ and speed of the bean (cm s^{-1}). Error bars represent the standard deviation of measurement ($N = 12$).

the landscape with a desired temperature less than the center temperature. Their initial orientation is randomly generated such that they move out from the center of the landscape in random directions, taking *run-steps-before-tumble* number of steps before performing a tumbling maneuver.

The beans step (or move) to an adjacent cell at every time step. During the tumbling maneuver, the beans take a step to the cell directly in front of them, followed by a 15° change in their orientation, followed by another step, etc. During each step, they record a sensed temperature, which differs from the actual cell temperature as described above (equation 6). In doing so they complete a circular loop. The lowest of the sensed temperatures then dictates the direction they head next for *run-steps-before-tumble* number of steps before performing another tumbling maneuver. With each step their stored temperature either increases or decreases based on equation (5).

5.1. Random tumbling generates optimal trajectories

A discussion on the rule set used by the bean during tumbling completes the model description. Several sets were tested before arriving at two final candidates that produce simulation results with emergent behavior similar to that observed in figure 4(b). These two include a set whereby the tumbling is always performed by changing heading to the right side of the bean, and a set whereby the bean first randomly selects if the tumbling will be right or left turning. Note that once decided, the entire tumbling event occurs using the decided direction.

Typical results from both sets appear in figures 8(b) and (c) for the robot and figures 8(e) and (f) for the numerics. Figure 8(d) shows a third comparison result in which the beans execute random walks. Each of the subfigures was

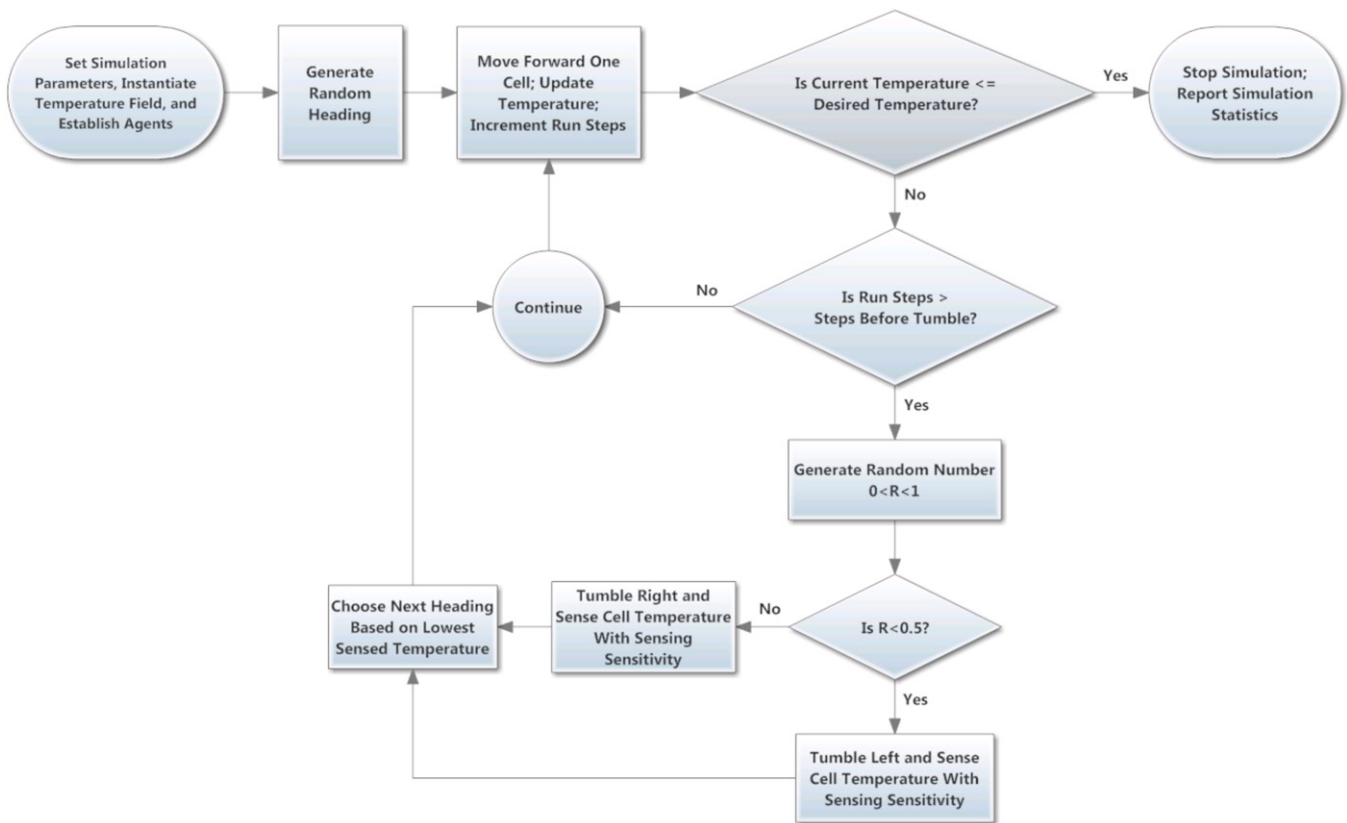


Figure 7. Symbolic flow chart of the jumping bean search algorithm.

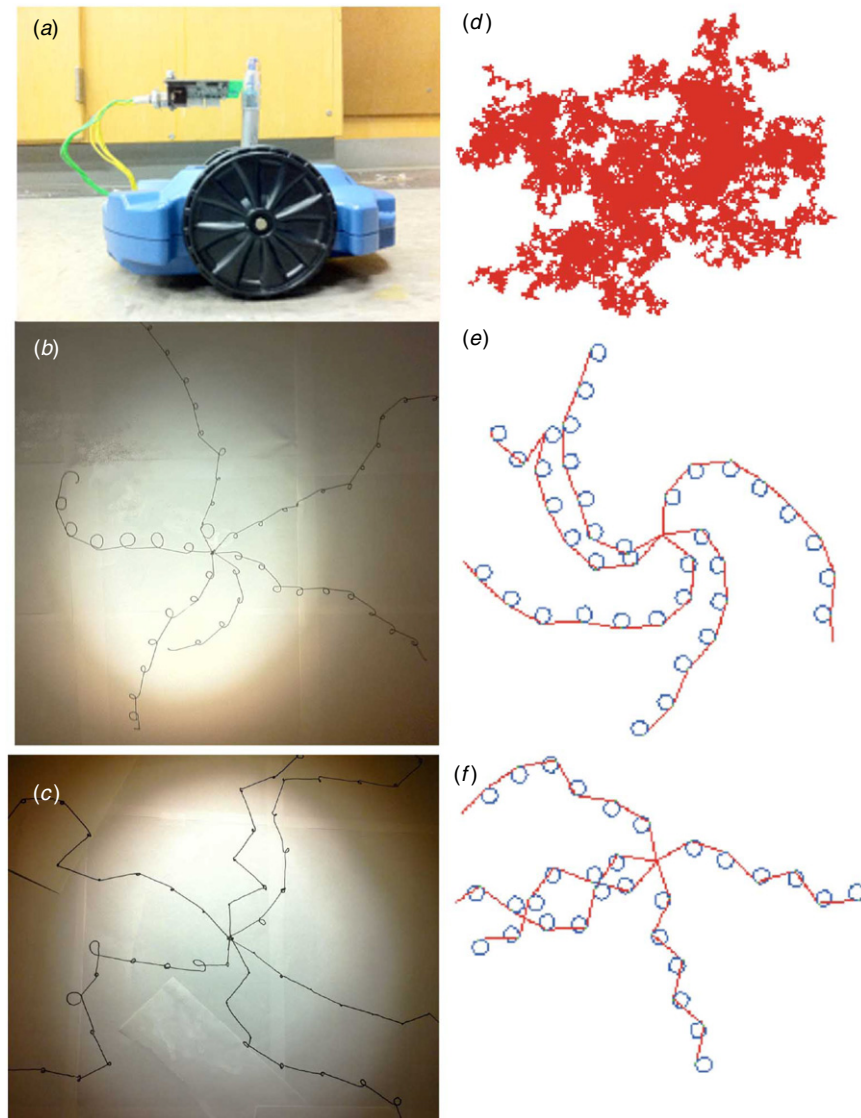


Figure 8. (a) Wheeled Scribbler robot modified to test the jumping bean search algorithm. The repositioned light sensor to reduce the influence of the robot's shadows. (b–f) Trajectories of the robot (black) and simulation (red) in a radial linear gradient of light. (b, e) Right-turning tumbles only show emergent behavior such as spirals. These spiral trajectories are non-optimal. (c, f) Here, random decisions are made about left- and right-turning tumbles, showing generally radial trajectories which are optimal in this setting. (d) A random walk approach is clearly poor for exiting a radial linear gradient in temperature.

generated using runs of the robot or numerical 'bean' sensing with 100% accuracy. Trials were run until the beans came to rest with a temperature state below their desired temperature. For the robot, trajectories are colored black. In the simulation, trajectory steps associated with running are colored red, while tumbling steps are colored blue.

The first rule set, assuming only right-handed turns, results in interesting emergent behavior (see figures 9(b) and (e)): on the radially graded temperature surface, the robot and simulated beans both take spiral-like trajectories that exhibit a high degree of smoothness. These spiral trajectories are relatively inefficient since they do not result in the optimal, radial trajectory. The spiral bias is due to right-handed turns not providing the bean the ability to sense temperatures to the left of their trajectory. As a result, beans are unable to move in the optimal radial paths. The resulting inefficiency offers

one explanation for why the beans in the experiment (figure 4) are observed to tumble both to the left and to the right: this is ultimately more efficient thermotaxis.

A rule set whereby the tumbling direction is random is given in figures 9(c) and (f). The trajectories are generally less smooth than the right-turning results, as shown by the jagged patterns. However, they more closely follow an optimal, radial trajectory. The observed switchbacks in the subfigure are consistent with those observed by the larva in figure 4.

One qualitative difference worth pointing out exists between the simulation and the experiments. Modeled tumbling trajectories exhibit strict circular patterns, while the experiments exhibit tumbling trajectories with more of a loop-like character. Both tumbling trajectories result in the bias discussed above however, and so the qualitative difference

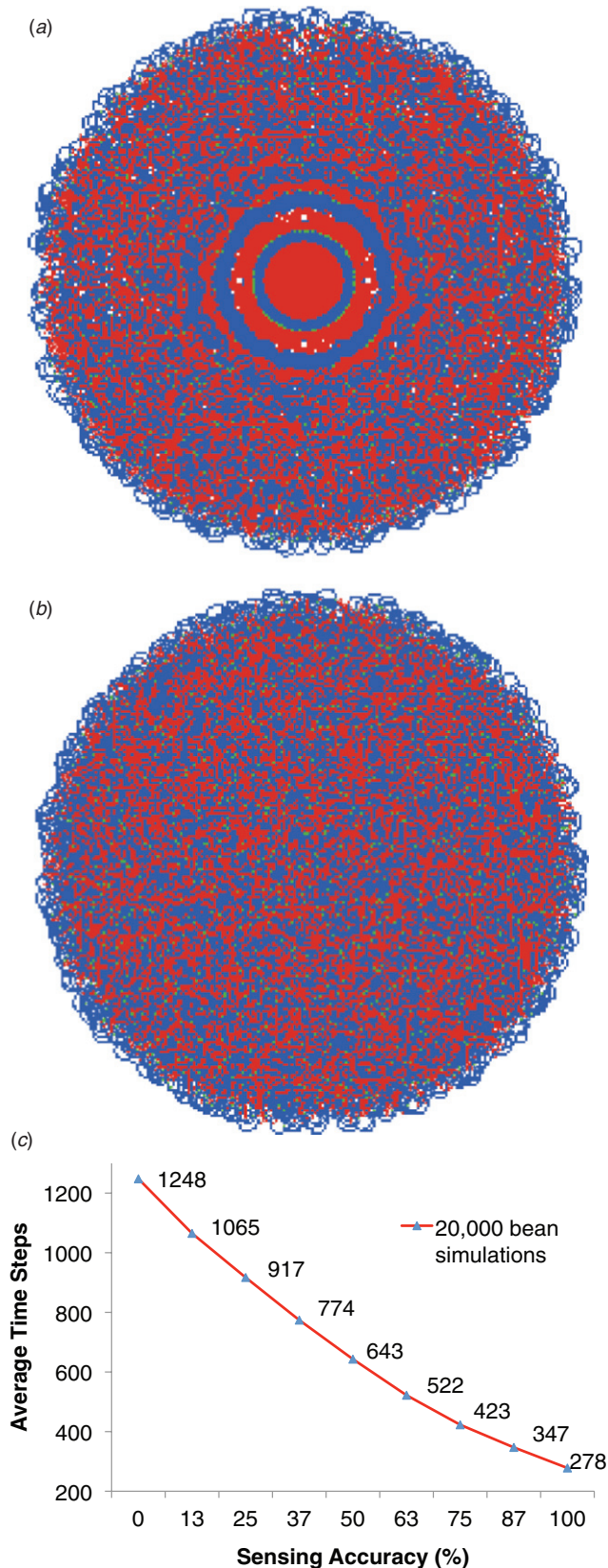


Figure 9. Simulation results showing the trajectories of 1000 beans with (a) perfect sensing ($S = 100$) and (b) zero-accuracy sensing ($S = 0$). (c) The average time to reach the bean's desired temperature as a function of sensing accuracy. 20 000 simulation runs were performed for each data point. For comparison, a random walk approach requires an average of 9600 time steps.

(circles vice loops) should have relatively little effect on modeled thermotaxis.

Finally, it is worth comparing the bean thermotaxis to a random walk, for which a simulation of a single bean is depicted in figure 8(d). Here, step size is a single grid spacing. It is clear from the comparison that the bean thermotaxis approach is far more efficient and near optimal for exiting a radial thermal gradient than randomly walking. The random-walk approach would be better for finding isolated shadows within the landscape, such as those generated by the shade of a tree's leaves.

5.2. Sensing accuracy

The model allows us to explore behavior or issues apart from bean thermotaxis that might be important in a bio-inspired application. One issue is the requisite sensing accuracy necessary to achieve effective thermotaxis. The effect of the sensing accuracy is explored in figure 9. The two extremes of sensing accuracy are first explored in figure 9 using 1000 beans: perfect and zero accuracy. Zero-accuracy sensing implies that the sensed temperature has a variance equal to the actual temperature: as a result, beans are effectively random walkers with a step size given by the run stage. The perfect sensing results in very little tracing back of the beans to the center of the domain, as evidenced by the coherent blue circular rings in figure 9(a). Recall that these blue rings result from tumbling, while red results from running. When a bean runs over a tumbling trajectory, it replaces the blue with a red cell (and vice versa). Patterns emerge in which the first two tumbling zones, and the third to some extent, survive as the beans head near-radially outward. Beyond that, the tumbling trajectories appear random. In contrast, the zero-accuracy trajectories in figure 9(b) appear random-like throughout the domain, without tumbling coherence, and with a distribution radius equal to that in figure 9(a).

The average time to reach a bean's desired temperature (one measure of effectiveness), as a function of sensing accuracy, is explored in figure 9(c). Simulations at each sensing accuracy were run using 20 000 beans. The average number of time steps necessary for the beans to achieve their desired temperature was then recorded for sensing accuracies ranging from 0% to 100%. The plotted curve shows a weak hyperbolic character that could be closely approximated by a linear fit. As expected, the least amount of time (278 steps) to achieve the desired temperature occurs with 100% sensing accuracy. However, a run-tumble approach with even 0% sensing accuracy leads to acceptable performance (in this example 1248 steps—roughly 4.5 times longer than perfecting sensing). This can be compared to a random walk, which yields an average of 9600 steps, or 34.5 times longer than perfect sensing.

6. Discussion and conclusion

We investigated the navigation and locomotion of the Mexican jumping bean experimentally, robotically and *in silico*. In our live bean experiments, we classified bean movements into three

types (rolls, jumps and flips) and measured the likelihood of each. We showed that flips were nearly 100 times less likely than rolls and jumps, and that this difference was consistent with the energy expenditure by the bean. In 2D tests comparing larva in and outside of its shell, we found that the seed casing impedes the larva's thermal sensing and locomotion, as shown by its increased speed when traveling outside its shell. We also raced the beans along a 1D track with a fixed heat source at one end. Using time-lapse photography, we recorded the bean's position along the track, finding that the beans increased body speed with increasing temperature gradients.

An important result from our study was that both bean and larva exhibit a run-and-tumble trajectory similar to bacteria (Berg 1993, Codling *et al* 2008). This run-and-tumble motion is also employed by a variety of other organisms. For instance, fruit fly motion is composed of straight-line movements punctuated by saccades in which they switch direction (Tammero and Dickinson 2002). In particular choosing straight-line distances according to Lévy flights is optimal for locating targets that are distributed randomly and sparsely (Reynolds and Frye 2007). As stated by Reynolds, 'A Lévy search strategy minimizes the mean distance traveled and presumably the mean energy expended before encountering a target. The strategy is optimal if the searcher is exclusively engaged in searching, has no prior knowledge of target locations and if the mean spacing between successive targets greatly exceeds the searcher's perceptual range.' An interesting open question is whether jumping bean movement probabilities also correspond to Lévy flights.

The locomotion of the Mexican jumping bean relies on rolling, which is rare in the natural world. Few animals rely on wheels rather than appendages (LaBarbera 1983), and fewer still do so from within an opaque shell. A few counterexamples exist, such as passive rollers that use wind and gravity to roll: these include the tumbleweed, rolling salamander and rolling spider (Armour and Vincent 2006, Full *et al* 1993). Active rollers can choose their direction of travel by inputting energy and steering: examples include the mother-of-pearl caterpillar and the stomatopod shrimp. A recent example of active rolling performed by a bio-inspired caterpillar robot is found in Lin *et al* (2011). Jumping beans, as we found in this study, along with jumping galls may also be considered to be active rollers.

We observed that the notch in the bean's shell increases its ability to ascend inclines and obstacles with respect to a spherical shell. This asymmetry increases the bean's cost of locomotion on flat terrain. Nevertheless, the asymmetry might benefit the design of spherical robots. For example, it is possible to form objects that are purely circular in one plane, but asymmetrical in another plane (such as a football), allowing for both increased maneuverability over objects and high efficiency over flat ground. The notch also helps allow the bean to increase traction during jumping and rolling. Although current rolling robots cannot yet hop, the use of a notch may enable these robots to do so.

Using our computational model, we were able to show that the search behavior of the bean can be mimicked using

relatively few rules. The simplicity of the jumping-bean search algorithm may be useful for designing navigation systems for small-scale robots (Melhuish and Lane 1999), such as solar-powered mechanical jumping beans for micro-robotics applications. For example, under strong light, a collection of such robots could show a 'hiding' response, by jumping randomly until the beans are hidden in the shadows of objects. The programming of the beans as agents is thus very simple: their only rule is to stop jumping once their preferred temperature is achieved. This suggests a very simple modality for detecting temperature gradients, and potentially a very cheap sensor, as we demonstrated in testing with a commercially available robot. Other gradients (chemical, light) could be sensed using this logic, and because of the simplicity of the hardware used, such behaviors may be applied for surveillance activities on the small scale.

Acknowledgment

The authors thank Z Zhang for helpful discussions.

References

- Alves J and Dias J 2003 Design and control of a spherical mobile robot *Proc. of the Institution Mechanical Engineers Part I: J. Syst. Control Eng.* **217** 457–67
- Armour R and Vincent J 2006 Rolling in nature and robotics: a review *J. Bionic Eng.* **3** 195–208
- Avallone E, Baumeister T and Sadegh A 2007 *Marks' Standard Handbook for Mechanical Engineers* (New York: McGraw-Hill)
- Berg H 1993 *Random Walks in Biology* (Princeton, NJ: Princeton University Press)
- Bhattacharya S and Agrawal S 2002 Spherical rolling robot: a design and motion planning studies *IEEE Trans. Robot. Autom.* **16** 835–9
- Bonabeau E 2002 Agent-based modeling: methods and techniques for simulating human systems *Proc. of the Natl Acad. Sci. USA* **99** 7280–7
- Codling E, Plank M and Benhamou S 2008 Random walk models in biology *J. R. Soc. Interface* **5** 813–34
- Full R J, Earls K, Wong M A and Caldwell R L 1993 Locomotion like a wheel?: backward somersaulting stomatopods *Nature* **365** 495
- Heckrotte C 1983 The influence of temperature on the behaviour of the mexican jumping bean *J. Therm. Biol.* **8** 333–5
- Herter K 1955 Über die orientierung der springbohen *Biol. Zentralbl.* **74** 565–79
- Incropera F, DeWitt D, Bergman T and Lavine A 2007 *Fundamental Of Heat and Mass Transfer* 6th edn (New York: Wiley)
- LaBarbera M 1983 Why the wheels won't go *Am. Nat.* **121** 395–408
- Lin H, Leisk G and Trimmer B 2011 Goqbot: a caterpillar-inspired soft-bodied rolling robot *Bioinspir. Biomim.* **6** 026007
- Melhuish C 1999 Controlling and coordinating mobile micro-robots: lessons from nature *IMECE 99: Proc. Int. Mechanical Engineering Congress and Exposition* (Nashville, TN)
- Reynolds A and Frye M 2007 Free-flight odor tracking in *Drosophila* is consistent with an optimal intermittent scale-free search *PLoS One* **2** 354
- Souman J, Frissen I, Sreenivasa M and Ernst M 2009 Walking straight into circles *Curr. Biol.* **19** 1538–42
- Sugiyama Y, Shiotsu A, Yamanaka M and Hirai S 2005 Circular/spherical robots for crawling and jumping

- Proc. of the IEEE Int. Conf. Robotics and Automation* vol 4 pp 3595–600
- Tammero L and Dickinson M 2002 The influence of visual landscape on the free flight behavior of the fruit fly *Drosophila melanogaster* *J. Exp. Biol.* **205** 327–43
<http://jeb.biologists.org/content/205/3/327>
- Wang Y and Halme A 1996 *Spherical Rolling Robot* Helsinki University of Technology ISBN 951-22-2990-0
- Wilensky U 1999 Netlogo <http://ccl.northwestern.edu/netlogo>
- Wolfram S 2005 Cellular automata *Modeling Chemical Systems Using Cellular Automata* ed L B Kier, P G Seybold and C-K Cheng (New York: Springer) pp 9–38